Pertanika J. Sci. & Technol. 26 (3): 1053 - 1066 (2018)

SCIENCE & TECHNOLOGY

Journal homepage: http://www.pertanika.upm.edu.my/

Distinct pH-dependent Aggregation of Citrate-Capped Colloidal Gold in Presence of Citrate Competitors

Fatemeh Javadi-Zarnaghi[1]*, Fahimeh Hosseini[2] and Dorsa Mohammadrezaei[3]

[1]Department of Biology, Faculty of Sciences, University of Isfahan, Isfahan, Iran
[2]Mechanical and Industrial Engineering Department, University of Toronto, Toronto, Canada
[3]Department of Chemical Engineering, Isfahan University of Technology, Isfahan, Iran

ABSTRACT

Many colorimetric biosensors utilise citrate-capped gold nanoparticles ($AuNP_{cit}$) in combination with functional macromolecules. Proper function of the utilised macromolecules is strongly dependent on the buffer systems. However, it is well known that solvents and buffers might cause aggregation of nanoparticles. A comprehensive and systematic investigation on the effect of buffer composition, concentration and pH on the aggregation of $AuNP_{cit}$ is reported in this study. Distinct aggregation behaviours were observed in acidic and basic pH. In acidic pH, the increase in pH, caused stabilisation of $AuNP_{cit}$, while in basic pH, the stability was dependent on the ionisation degree of the applied buffer. Theoretical analyses revealed that ionic buffer species act as citrate competitors and control aggregation of $AuNP_{cit}$. Understanding the fundamental principles of competition between citrate and buffer components allows scientists to choose orthogonal conditions for development of gold nanoparticle-based biosensors which guarantee stability of gold nanoparticles and proper folding of macromolecules simultaneously.

Keywords: Aggregation, citrate buffer, gold nanoparticles, Good's buffers, Henderson-Hasselbach equation

INTRODUCTION

Detecting threatening substances and microorganisms is an essential requirement for human health and environmental care. Nowadays, biosensors play an important role on detection of such molecular hazards. As defined by the international union of pure and applied chemistry (IUPAC), biosensors are "chemical sensors in which the recognition system utilizes a biochemical mechanism". The recognition elements of biosensors are

ARTICLE INFO

Article history:
Received: 12 October 2017
Accepted: 17 January 2018

E-mail addresses:
fa.javadi@sci.ui.ac.ir (Fatemeh Javadi-Zarnaghi)
fahimeh.hosseini93@gmail.com (Fahimeh Hosseini)
dmohammadrezaie@gmail.com (Dorsa Mohammadrezaei)
*Corresponding Author

ISSN: 0128-7680

usually composed of peptides (Tang et al., 2012), enzymes, antibodies (Lazcka et al., 2007) and single stranded DNAs such aptamers and (deoxy)ribozymes (Endo et al., 2005; Zhao et al., 2008). Each of these macromolecules requires specific and distinct buffer with defined pH, concentration and composition for proper fold and function.

Biosensors benefit from several methods of data acquisition including colorimetric readouts (Chen et al., 2015). Most colorimetric methods depend on special characteristics of gold nanoparticles (AuNPs, colloidal gold). Gold nanoparticles have an intensive and distinctive colour which is due to the localised surface plasmon resonance (LSPR) effect (Liu et al., 2006; Petryayeva et al., 2011). The position of the LSPR peak in the visible spectrum depends on the shape, size and dispersity of the gold nanoparticles in the colloid. A well-dispersed AuNP colloid bears an LSPR peak around 510-530 nm and is red (Petryayeva et al., 2011). The peak intensities are reduced and are shifted to 620-670 nm upon aggregation. As a result of such red-shift, the colour of the colloid turns blue (Niu et al., 2014).

Since many colorimetric AuNP-based biosensors harness the colour of the colloid as the readout of the sensor, the aggregation of gold nanoparticles and thus the LSPR red-shift must be monitored strictly. There are two strategies to implement the colour-change of the AuNP-based biosensors. In one strategy, the gold nanoparticles are designed to aggregate upon presence of the target molecules. In the others, the target stabilises the gold nanoparticles and inhibits the aggregation (Lonne et al., 2014). In either of the strategies, it must be guaranteed that aggregation of gold nanoparticles does not occur spontaneously.

The gold nanoparticles used in many of reported biosensors are synthesised by a well-known method of reduction of hydrogen tetrachlorocuprate (III) with citrate. The colloids of citrate-capped gold nanoparticles ($AuNP_{cit}$) are prone to aggregate when subjected to extra additives. It is well known that $AuNP_{cit}$ aggregates in presence of solutions of chlorides and other halides (Zhang et al., 2014). Aggregation of gold nanoparticles was also reported in presence of organic molecules such as urea, thiourea, glutathione and ethanolamine (Chegel et al., 2012).

Susceptibility of $AuNP_{cit}$ to aggregation in the presence of additives complicates choosing a proper buffer system. In one hand, it must be assured that undesired aggregation of gold nanoparticles does not ensue with non-target species of the buffer. On the other hand, the buffer system must accommodate functional folding of the macromolecules of the biosensor. Hence, applying orthogonal conditions with defined buffer component, concentration and pH is crucial for development of colorimetric biosensors. The orthogonal condition must support proper folding and activity of the macromolecule and simultaneously, must not induce gold nanoparticle aggregation.

In this respect, there is a demand for comprehensive and systematic investigations of the effects of the common buffer systems on the aggregation of $AuNP_{cit}$, which has not been studied, to the best of our knowledge.

A handful of buffers over the range of pH 3.0-9.0 were selected to be analysed in this study. The buffer components have been either citrate or members of Good's buffer that are of valuable interest in pharmacy (March, 2004), industry (Zhou et al., 2010) and biosensor development (Jiang et al., 2008). Citric acid buffer systems are one of the common buffers for development of biosensors (Ang et al., 2015). Citrate buffer is a carboxylic acid buffer with three acidic protons that compose a continues range of buffering system from ca. 2.0 to

7.0. Good's buffers (Good et al., 1972) are N-substituted taurine or glycine molecules and have specific properties which prioritize them as biological buffers. Solubility, non-toxicity, little absorption within UV and visible spectrum and less interaction with metal ions are some advantageous properties of Good's buffers. Moreover, the p*K*a values of Good's buffers are beneficially less dependent on the concentration of the buffer and temperature.

Here, the effect of citrate and several Good's buffers with different pH is presented on the aggregation of citrate-capped colloidal gold (Figure 1). An aggregation constant is reported for each condition that help molecular biologists to decide most suitable buffer for individual biosensors. It is demonstrated that the aggregation of citrate-capped gold nanoparticles follows distinct mechanisms in acidic and basic pH. Theoretical explanations are included to understand the particular response of the gold nanoparticles to various buffer systems.

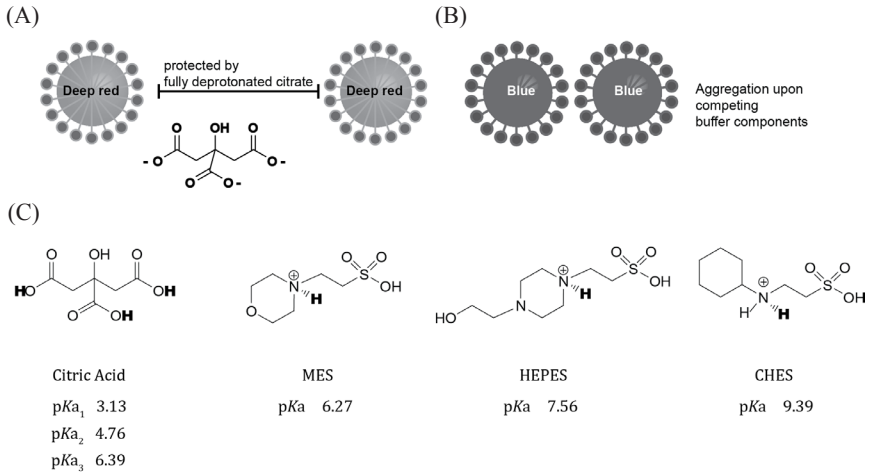

Figure 1. (A) Schematic illustrations of the coordination of the positive charges at the surface of gold nanoparticles with citrate species. (B) Shcematic representation of the aggregated form of gold nanoparticles. (C) Illustration of the buffers used in this study in their fully protonated form. The protons for which the pKa values are marked with bold letters. MES: 2-(N-Morpholino)ethanesulfonic acid, CEHS: 2-(Cyclohexylamino) ethanesulfonic acid, HEPES: 4-(2-Hydroxyethyl)piperazine-1-ethanesulfonic acid

MATERIALS AND METHODS

Chemicals

Good's buffers i.e. 2-(N-Morpholino)ethanesulfonic acid hydrate (MES), 4-(2-Hydroxyethyl) piperazine-1-ethanesulfonic acid (HEPES) and 2-(Cyclohexylamino)ethanesulfonic acid (CHES), citric acid monohydrate, trisodium citrate dehydrate, sodium hydroxide and hydrogen tetrachlorocuprate (III) (HAuCl4) were purchased from Sigma-Aldrich.

Synthesis of Gold Nanoparticles

All glassware were washed with aqua regia (3:1 concentrated HC_l:HNO_3) for 30 min and subsequently rinsed with generous amount of deionised water and then ultrapure water (18.2

$M\Omega \cdot cm^{-1}$). Synthesis of gold nanoparticles was based on earlier studies (Liu et al., 2006). To begin the synthesis, 100 ml of 1 mM $HAuCl_4$ was brought to reflux on a heater with a magnetic stirrer, consequently 10 ml 38.8 mM sodium citrate was added. The change from pale yellow to deep red was observed within one minute. The system refluxed for further 20 minutes before it cooled down to room temperature while still stirring.

Dynamic Light Scattering (DLS) Measurement

DLS was measured on a DynaPro (Wyatt Technology) with diluted synthesised gold nanoparticles. The dilution factor was 1:100. The laser intensity of the instrument was set to 80% and measurements were performed in 2 ml cuvettes.

Buffer Preparation

Citrate buffer pH 3.0 and 5.0, MES buffer pH 6.0, HEPES buffers pH7.0, 7.5 and 8.0 were prepared by dissolving appropriate amount of buffer in 100 ml of ultrapure water. After pH adjustment with 2 N NaOH, the volume adjusted to 200 ml to achieve 1 M buffer solutions. CHES buffers pH 9.0, 9.5 and 10.0 were prepared in 0.5 M stock concentration based on the same procedure.

Titration Procedure

Measurements were performed in a total volume of 1 ml. To 250 microlitre of citrate-capped AuNP, appropriate amount of ultrapure water and appropriate amount of the concentrated buffer were added with the stated order. Final concentrations of buffers were 250, 200, 150, 100, 80, 50, 20, 10 and 5 mM. The mixtures gently pipetted up and down and incubated for 30 minutes at room temperature. The spectra of AuNPs incubated with buffers were measured in the visible range of 450 nm to 750 nm in a quartz cuvette. Titration series for each buffer composition and pH were repeated three times with three stock buffer solutions which were prepared independently.

Data Analysis

The ratio of absorbance at the peak of aggregated forms (620 nm) to the absorbance of the peak of non-aggregated form (520 nm) is usually considered as a measurement for aggregation (Mei et al., 2013; Song et al., 2012; Song et al., 2011). For each individual spectrum, the absorbance at 620 nm was divided to the absorbance at 520 nm to reach the $A_{620\ nm}/A_{520\ nm}$

ratio (Absorbance ratio, AR) as a measure of aggregation. The outcome was plotted as bar graphs. To eliminate the background, progress of aggregation (PAG) was defined as equation 1:

$$\mathrm{PAG} = [A_{620\,nm}/A_{520\,nm}] - [A_{620\,nm,\ no\ buf.}/A_{520\,nm,\ no\ buf.}] \quad (1)$$

The PAG Values were plotted against the concentration of the buffer system as scatter. The Hill equation was fitted to the data (equation 2).

$$\mathrm{PAG} = \frac{\mathrm{PAG}_{max}[buf.]^n}{K_{Agg.}+[buf.]^n} \quad (2)$$

In equation 2, PAG is a measure of an increase in the absorbance ratio (AR) and shows progress of aggregation. $KA_{gg.}$ is aggregation constant. The concentration of buffer is denoted as [*buf.*] and the letter n, indicates the Hill constant which is a measure of cooperativity.

RESULTS

Dynamic light scattering (DLS) or photon correlation spectroscopy (PCS) is a physical method that is usually utilised for measuring the size distribution of nano-scale particles in a suspention or macrocmolecules in solutions (Stetefeld et al., 2016). The size distribution of the synthesised gold nanoparticle was characterised by DLS. The population mode of particles in the synthesised gold colloid was 11 nm and 90% of the particles had the size distribution between 6-14 nm.(Figure 2A). The spectrum of the citrate-capped synthesised AuNP had a localised surface plasmon resonance peack at 520 nm (Figure 2B). The conditions at which buffers cause aggregation were observed. Such aggregations are non-target and must be avoided in development of biosensors. As an example, presence of 250 mM citrate buffer pH 5.0 caused a red-shift in LSPR peak (Figure 2C). The LSPR band shift is usually due to a reflection of aggregaion of the gold nanoparticles (Mei et al., 2013). The-red shift in the absorption spectra was also visible with the change in the colloidal gold from red to blue/purple. Such buffer-induced red-shifts that is independent of the presence of specific targets must be avoided during development of biosensors. In this study, comprehensive studies were performed by titration experiments. Titration of the citrate-capped gold nanoparticles with individual buffers resulted in a different degree of aggregation. The aggregation level depended on the composition and final concentration of buffers. The LSPR band shifted from 520 nm to 620 nm when high concentrations of buffers were present.

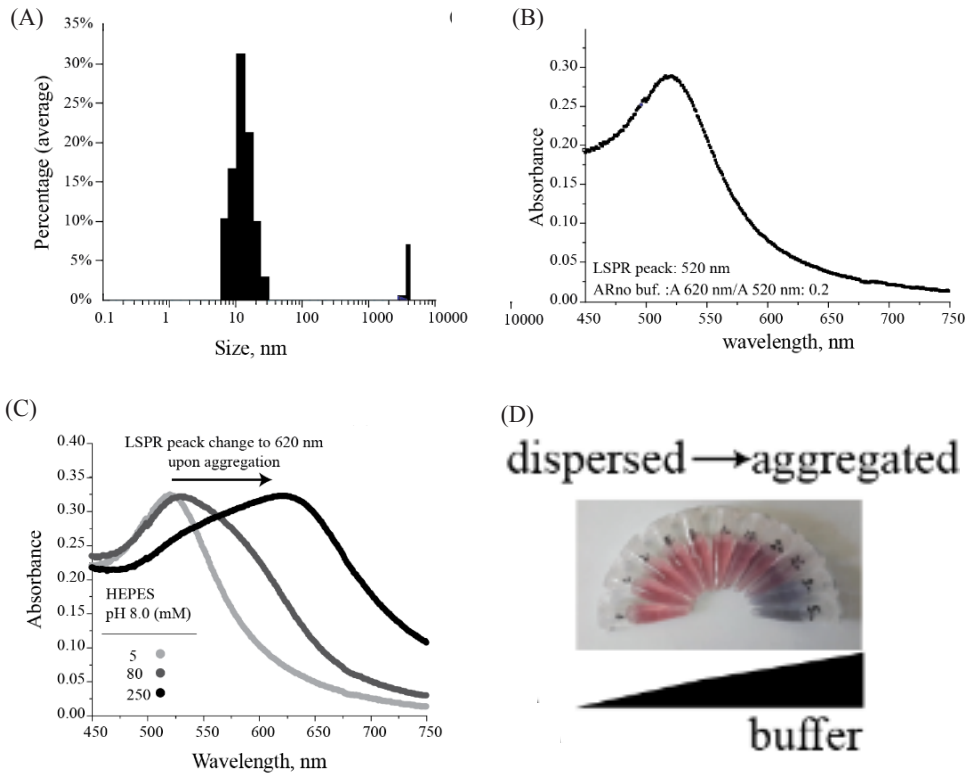

Figure 2. (A) Dynamic Light Scattering (DLS) data for the synthesized citrate-capped gold nanoparticles in this study. (B) The visible spectrum of the synthesised nanoparticle (4 times diluted sample). (C and D) Representative spectra and colloid color change upon presence of the buffers. The LSPR peak shifts toward longer wavelength upon aggregation and the colour of the colloid changes to blue

Increase in the ratio of the spectral absorption at 620 nm to the spectral absorption at 520 nm (A_{620} nm/A_{520} nm, absorbance ratio, AR) is a measure of aggregation (Mei et al., 2013; Song et al., 2012; Song et al., 2011). The AR had a background amount which was the AR for the monodisperesed citrate-capped gold nanoparticles in the absence of any additive ($AR_{\text{no buf.}}$). The synthesised gold nanoparticles in this study had an $AR_{\text{no buf.}}$ of 0.20 (Figure 2B). Figure 3 illustrates the AR for each condition as a measure of aggregation level. As AR increases, species that are transformed from monodispersed to aggregate form get higher percentage of the population. At AR above 1.0 the population of aggregated forms are predominated. Thus, conditions at which AR is above 1.0, should be avoided in the development of biosensors.

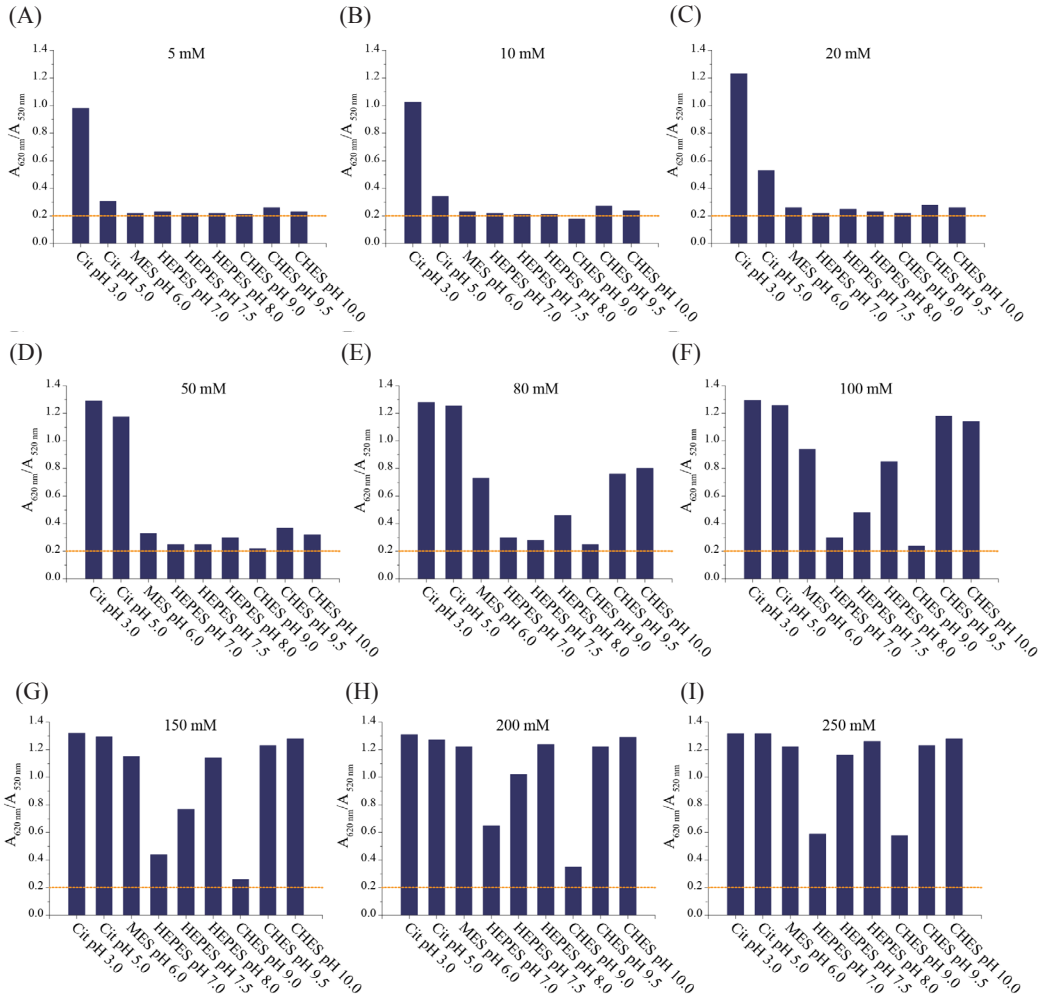

Figure 3. The A_{620 nm}/A_{520 nm} (AR) as a measure of aggregation level of citrate-capped gold nanoparticles in different pH from 3.0 to 10.0. Concentration of the applied buffer is increased from 5 mM to 250 mM from pannels a to i. The background AR is shown with the dashed orange lines

Addition of the citrate buffer pH 3.0 to the AuNP colloid caused a severe aggregation even at low concentrations. At 5 mM pH 3.0 citrate buffer, the AR was 0.98 which was ca. 5 times higher than synthesised gold nanoparticle in the absence of any additive. Increasing the concentration of citrate buffer pH 3.0 to 250 mM increased AR ratio to 1.31. Citrate buffer pH 5.0 showed less harsh effects. Presence of 5 mM pH 5.0 citrate buffer had almost no effect on AR. Increasing the concentration of citrate buffer pH 5.0 to 20 mM resulted in AR of 0.52 which was ca. 2.5 times higher than synthesised gold nanoparticle. At 250 mM this ratio reached 1.31.

2-(N-Morpholino)ethanesulfonic acid (MES) buffer provided the pH 6.0 for this study. In the presence of MES buffer pH 6.0, the colloidal gold resisted for aggregation up to 80 mM. Increasing the concentration of MES buffer pH 6.0 to 250 mM resulted in AR ratio of 1.22 which was slightly less severe change compared with what was observed with citrate buffers pH 3.0 and 5.0.

Presence of 4-(2-Hydroxyethyl)piperazine-1-ethanesulfonic acid (HEPES) buffer pH 7.0 was best tolerated even at relatively high concentrations. The AR reached only 0.54 when the concentration of HEPES buffer pH 7.0 was raised to 250 mM. Increasing the pH of HEPES buffer to 7.5 and 8.0 returned sensitivity of the gold nanoparticles. The AR reached 1.16 and 1.26 at 250 mM buffer for pH 7.5 and 8.0 respectively. However, the effect was only visible in concentrations higher than 80 mM. Notably, although at 250 mM the HEPES pH 7.5 and 8.0 almost showed the same effect as citrate pH 3.0 and 5.0 and MES pH 6.0, the instability of gold nanoparticle colloids was less noticeable for lower concentrations of HEPES buffers.

Changing the buffer composition to 2-(Cyclohexylamino)ethanesulfonic acid (CHES) had a stabilising effect. CHES buffer pH 9.0 showed very similar effect as HEPES buffer pH 7.0. The AR at 250 mM CHES buffer was 0.58. In other words, pH 9.0 was better tolerated than pH 8.0, keeping in mind that the buffer composition was changed from HEPES to CHES. In presence of CHES buffer pH 9.5 and 10 the sensitivity returned and the AR reached 1.03 and 1.08 at 250 mM respectively (Figure 4).

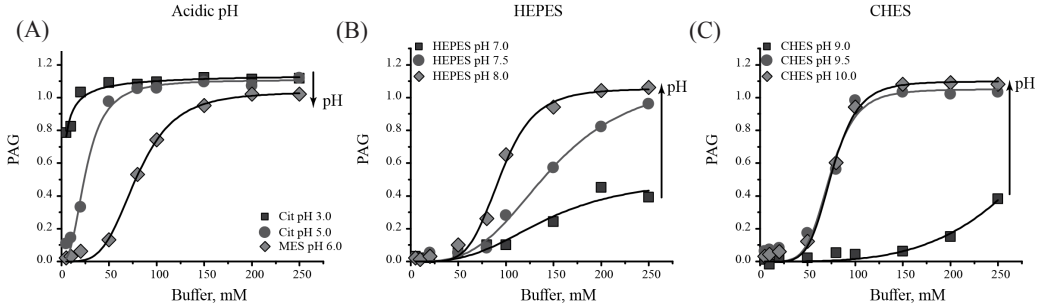

Figure 4. Progress of aggregation (PAG) of citrate-capped gold nanoparticle colloids in the presence of increasing concentrations of buffers. The aggregation phenomena was distinct in acidic and basic pH. Additionally, changing the buffer component from HEPES to CHES has a stabilising effect

In the next step, progress of aggregation (*PAG*) was defined as an increase in the AR. Aggregation constant ($K_{agg.}$) as the concentration of buffer at which PAG reaches half of its maximum value. Figure 4 illustrates the titration curves. The $K_{agg.}$ and Hill coefficient for each buffer composition and pH were achieved by fitting the Hill equation and are shown in Table 1.

Table 1
Fit values of the Hill curve for the PAG

Buffer	Citrate		MES		HEPES		CHES		
pH	3.0	5.0	6.0	7.0	7.5	8.0	9.0*	9.5	10.0
PAG_{max}	1.15	1.11	1.04	0.51	1.13	1.06	n.d.	1.05	1.10
$K_{Agg.}$, mM	2.24	25.88	79.33	142.18	147.92	94.26	n.d.	73.77	75.92
Hill constant	0.84	2.54	3.99	3.05	3.28	5.31	n.d.	5.49	5.68

* Fit values of CHES pH 9.0 are not defined since the data did not reach to a plateau of aggregation level within the concentration range

Distinct observations were achieved with acidic and basic pH (Figure 4A vs. B and C). In addition, exchanging the buffer system from HEPES to CHES caused a clear difference (Figure 4B and C). From pH 3.0 to 6.0, stability of gold nanoparticles was increased with an increase in pH. From pH 7.0 to 8.0, with HEPES buffer stability was decreased with an increase in pH. Changing the buffer from HEPES 8.0 to CHES pH 9.0, had a stabilising effect. From pH 9.0 to 10.0, again the stability was decreased with an increase in the pH.

In the acidic buffers, increasing pH (from pH 3.0 to 6.0, Figure 4A), had almost no effect on PAG_{max}, while K_{agg} was increased from ca. 2 mM to 80 mM. Constant PAG_{max}, with increased K_{agg}, was attributed as increased stability of the gold nanoparticles. The cooperativity of aggregation phenomenon (n) was also increased. Aggregation at near-neutral pH was more dependent on the concentration of the buffer.

Despite acidic buffers, increasing pH with HEPES buffer (from pH 7.0 to 8.0, Figure 4B), was destabilising. PAG_{max} was increased from ca. 0.5 to ca. 1.1, while K_{agg} was decreased from ca. 140 mM to ca. 94 mM. The cooperativity of aggregation was increased upon increase in the pH. Hence, aggregation at higher pH was shown to be dependent on the concentration of the buffer.

Changing HEPES to CHES buffer caused stability of the colloidal gold. However, increase in pH with the CHES buffer had the same effects as with the HEPES buffer i.e. stability decreased upon increase in pH (Figure 4C).

In summary, distinct effects on the stability of colloidal gold upon increase in pH was observed. In acidic pH, the citrate-capped gold nanoparticles were stabilised when the pH increased. The effect was independent of the used buffer. In contrast, in basic pH, increased pH with a unique buffer resulted in increased instability. Finally, the stability of the colloidal gold was strongly dependent on the buffer type and concentration.

DISCUSSION

In this study, citrate-capped gold nanoparticles were subjected to increasing concentrations of various buffers. Citrate buffers were chosen for highly acidic pH (3.0-5.0). Good buffers were chosen for pH 6.0 and above. A different pattern of aggregation was observed for acidic and basic pH. It can be hypothesised that "accumulation of Cit^{3-} and its competitors" control such distinctive observations. Citrate-capped gold nanoparticles are best stabilised when the concentration of fully deprotonated form of citrate (Cit^{3-}) is at maximum. At very acidic pH, protonated forms of citrate are present which cannot coordinate at the surface of the gold nanoparticle. Hence, the colloid is sensitive to buffer moieties, even at very low concentrations. In pH above the pKa$_3$ of citrate (basic pH), all citrates are in the fully deprotonated form (Cit^{3-}) which supports maximum stability for gold nanoparticles. However, within this pH range, the deprotonated forms of the applied buffers compete with the Cit^{3-}. At pH above pKa of the applied buffer, the competition is in favour of buffer competitors since more deprotonated species of buffer are available to compete with Cit^{3-}.

Such competitions are explained below. Citric acid has three acidic functional groups. Calculating exact percentage of citric acid ionised species with Henderson-Hasselbach equation (H-H) supports the hypothesis of this study. H-H equation defines the relationship between pH,

p*K*a and the logarithmic ratio of deprotonated form of an acid to its protonated form. Based on H-H equation, three constant values (Q_1-Q_3) are defined as the ratios of deprotonated to protonated forms of citrate. In addition, Q_4 is defined as total concentration (100%) of citrate species (equations 3-6).

$$Q_1 = CitH_2^-/CitH_3 = 10^{(pH-pKa_1)} \quad (3)$$

$$Q_2 = CitH^{2-}/CitH_2^- = 10^{(pH-pKa_2)} \quad (4)$$

$$Q_3 = Cit^{3-}/CitH^{2-} = 10^{(pH-pKa_3)} \quad (5)$$

$$Q_4 = CitH_3 + CitH_2^- + CitH^{2-} + Cit^{3-} = 100\% \quad (6)$$

The four equations above are solved with a linear algebraic method to achieve exact percentage of each of the deprotonated form of citrate at any desired pH (equations 7-10). The theoretical percentage of each citrate species at given pH in this study is calculated using these equations (Table 2).

Table 2
Calculated percentage of each citrate species at pH used in this study

	pH	$CitH_3$%	$CitH_2^-$%	$CitH^{2-}$%	Cit^{3-}%
acidic	3.0	57.006	42.259	0.734	0.0003
	5.0	0.478	35.434	61.578	2.508
	6.0	0.005	3.927	68.259	27.807
neutral	7.0	1.53E-05	0.113	19.686	80.199
	7.5	5.59E-07	0.013	7.202	92.784
	8.0	1.86E-08	0.001	2.395	97.602
basic	9.0	1.90E-11	1.41E-05	0.244	99.755
	9.5	6.02E-13	1.41E-06	0.077	99.922
	10.0	1.90E-14	1.41E-07	0.024	99.975

$$CitH_3 = Q_4/(1 + Q_1 + Q_1Q_2 + Q_1Q_2Q_3) \quad (7)$$

$$CitH_2^- = Q_1Q_4/(1 + Q_1 + Q_1Q_2 + Q_1Q_2Q_3) \quad (8)$$

$$CitH^{2-} = Q_1Q_2Q_4/(1 + Q_1 + Q_1Q_2 + Q_1Q_2Q_3) \quad (9)$$

$$Cit^{3-} = Q_1Q_2Q_3Q_4/(1 + Q_1 + Q_1Q_2 + Q_1Q_2Q_3) \quad (10)$$

As shown in Table 2, theoretically, at pH 3.0, 57% of citrate is in the fully protonated form ($CitH_3$), 42% is di-protonated ($CitH_2^-$), 0.73% mono-protonated ($CitH^{2-}$) and only 0.0003% is in the fully deprotonated format (Cit^{3-}). In contrast to pH 3.0, at pH 7.0, less than 0.00002

% is fully protonated, 0.11 % is di-protonated, 19.7% is mono-protonated and 80% of the citrate is fully deprotonated. As it is clear, the species of Cit^{3-} accumulates upon increase in pH as the concentration of deprotonated forms increases from pH 3.0 to 7.0. Notably, at basic pH, the concentrations of protonated species of citrate turn to be negligible.

The fully protonated form of citric acid cannot serve as the stabilising agent for colloidal gold. In contrast the citrate species with more negative charges better stabilises the colloidal gold. Therefore, accumulation of Cit^{3-} species proportionally, increases the stability of the colloidal gold and decreases aggregation level (Figure 5A and Figure 5B). For instance, at pH

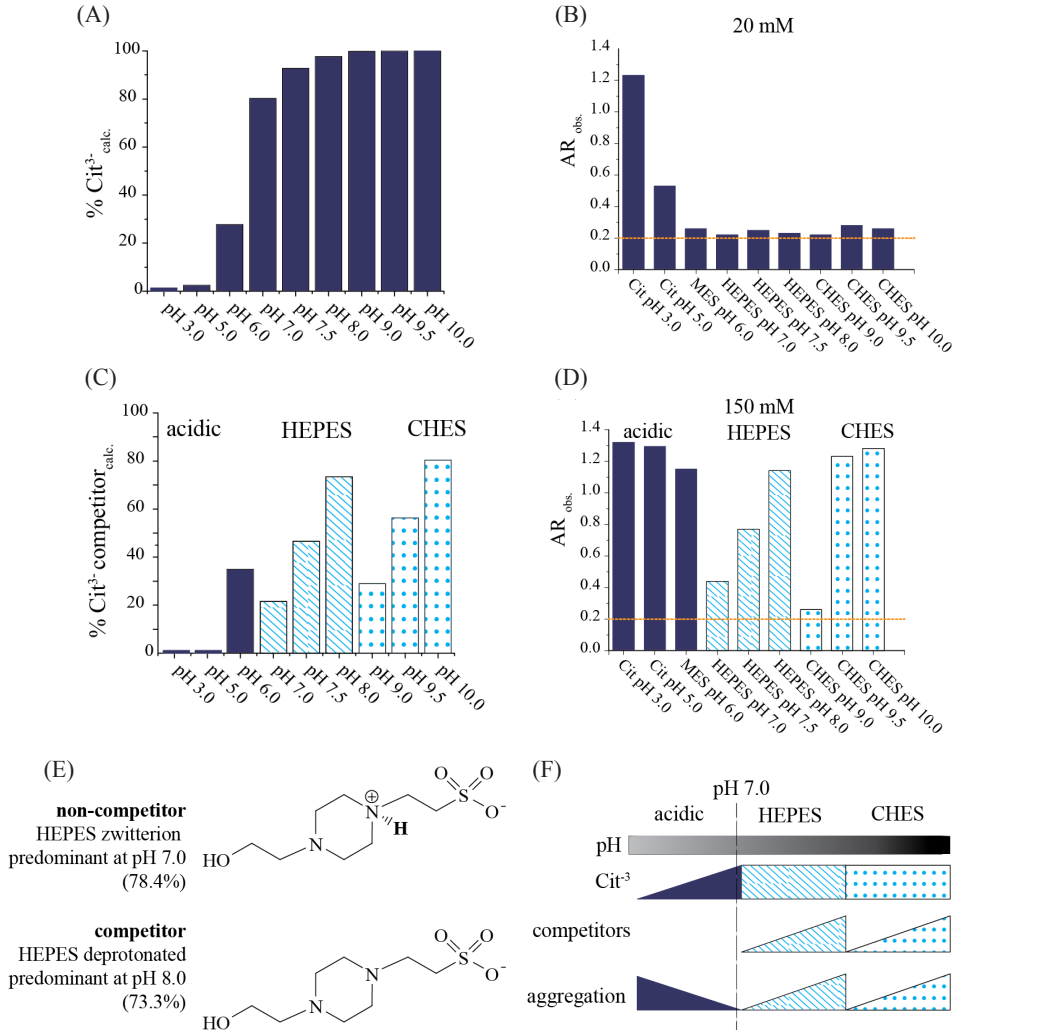

Figure 5. (A) Calculated percentage of cit3- species at given pH values. (B) Observed absorption ratio (AR obs.) of the citrate-capped gold nanoparticles in presence of 20 mM buffer of the indicated buffers. (C) Calculated percentage of the deprotonated forms of the MES, HEPES and CHES which act as competitors of the cit3-. (D) Observed absorption ratio (AR obs.) of citrate-capped gold nanoparticles in presence of 150 mM buffer of the indicated buffers. (E) The zwitterion and deprotonated forms of HEPES buffer. (F) A summary of the accumulation of cit3- and its competitors and their effects on the aggregation level of the citrate-capped gold nanoparticles. Acidic pH: solid fill; basic pH, HEPES: dashed fill; basic pH, CHES: dotted fill

3.0, most citric acid molecules are in the fully protonated form (57%) and cannot protect gold nanoparticles from aggregation and cause severe instability within the titration range (figure 3, first column in all panels).

At pH above 7.0, the concentration of Cit^{3-} is theoretically at its maximum and thus, a good stability is expected. However, new players come into play. As the pH increases the deprotonated form of the present buffer (HEPES or CHES) accumulates and competes with the Cit^{3-} (Figure 5E). Henderson-Hasselbach equation is used to calculate exact percentage of Good's buffers component at all pH that have been studied here (Table 3).

Table 3
Calculated percentage of deprotonated forms of the Good buffer that are used in this study

Used buffer	p*K*a	pH	HA	A-
MES	6.27	6	65.1	34.9
HEPES	7.56	7	78.4	21.6
		7.5	53.4	46.6
		8	26.6	73.4
CHES	9.39	9	71.1	28.9
		9.5	43.7	56.3
		10	19.7	80.3

Interestingly, the observed trend in the percentage of A^- (competitor form of the buffer) is proportional to the observed trend in aggregation of gold nanoparticles (Figure 5C and Figure 5D). As the pH increases from 7.0 to 8.0, the percentage of competitor form of HEPES (Figure 5E) is increased from 22% to 73%, which was accompanied by increase in aggregation (AR). Changing the buffer system to CHES, caused a drop in the percentage of the present competitor (since the p*K*a value of CHES is higher than HEPES), which was interestingly in concert with a stabilising effect on the gold nanoparticle, even though the pH is increased. As the pH increased from 9.0 to 10.0 the percentage of the competitor form of CHES increased from 28% to 80% and again, and this increase is reflected in the instability of gold nanoparticles. Competitor dependent displacement of citrate with halide ions was proposed to be the reason of aggregation by Zhang et al. (2014).

As expected, the effect of the competitors depends on the concentration of the used buffer. The higher concentration would increase competitor species to compete with the 3.9 mM Cit^{3-} which was present in the synthesised gold nanoparticles. The dependence of the competitor effect on the concentration of the used buffer was also well reflected in the Hill constants of the fit curves in titration experiments.

Altogether, titration of gold nanoparticles with different buffer composition, pH and concentration, revealed that the stability of the citrate-capped gold nanoparticles is dependent on all three items. Buffer type, the pH of the buffer and its concentration all can affect aggregation. In acidic pH, the accumulation of Cit^{3-} is the major player, since no competitor is present. Therefore, stability is increased upon increases in pH. In basic pH, stability us a

dependent on the competitor concentration. Accumulation of competitors causes aggregation of gold nanoparticles.

CONCLUSION

This is a comprehensive and systematic study on the aggregation of the sensitive citrate-capped gold nanoparticles in presence of generally used buffers in molecular biology and biochemistry. It is shown the stabilisation of gold nanoparticles that are capped with citrate is dependent on both the pH and the component of the buffer. In acidic conditions, the higher pH, forms higher ratio of Cit^{3-} in comparison to other citrate ionisation states. Hence, as the pH approaches to 7.0, the gold nanoparticles are better stabilised. In basic buffers, however, pH is not the sole ruler of the system for aggregation and at pH above 7.0, the ionisation degree of the applied buffer has a major impact on the spontaneous aggregation of the gold nanoparticles. This study promotes development of colorimetric biosensors that are based on gold-nanoparticles and allows scientists to better decide for the concentration and pH of the buffer, which prevents non-desired aggregation of the gold-nanoparticle and simultaneously, is compatible for the folding of their biomolecules.

LIST OF ABBREVIATIONS

Localised surface plasmon resonance (LSPR)
Gold nanoparticles (AuNP)
Progress of aggregation (*PAG*)
A620 nm/A520 nm, absorbance ratio (AR)

ACKNOWLEDGMENTS

The financial support provided by University of Isfahan is gratefully acknowledged. The authors wish to thank Mr. Hossein Golzar for providing some of the chemicals.

REFERENCES

Ang, L. F., Por, L. Y., & Yam, M. F. (2015). Development of an amperometric-based glucose biosensor to measure the glucose content of fruit. *PLoS One, 10*(3), e0111859. doi: 10.1371/journal.pone.0111859

Chegel, V., Rachkov, O., Lopatynskyi, A., Ishihara, S., Yanchuk, I., Nemoto, Y., … & Ariga, K. (2012). Gold nanoparticles aggregation: Drastic effect of cooperative functionalities in a single molecular conjugate. *The Journal of Physical Chemistry C, 116*(4), 2683-2690. doi: 10.1021/jp209251y

Chen, G., Guo, Z., Zeng, G., & Tang, L. (2015). Fluorescent and colorimetric sensors for environmental mercury detection. *Analyst, 140*(16), 5400-5443. doi: 10.1039/c5an00389j

Endo, T., Kerman, K., Nagatani, N., Takamura, Y., & Tamiya, E. (2005). Label-free detection of peptide nucleic acid-DNA hybridization using localized surface plasmon resonance based optical biosensor. *Analytical Chemistry, 77*(21), 6976-6984. doi: 10.1021/ac0513459

Good, N. E., & Izawa, S. (1972). Hydrogen ion buffers. [Comparative Study]. *Methods in Enzymology, 24*, 53-68.

Jiang, Z., Liang, A., Li, Y., & Wei, X. (2008). Immunonanogold-catalytic Cu_2O-enhanced assay for trace penicillin G with resonance scattering spectrometry. *IEEE Trans Nanobioscience, 7*(4), 276-283. doi: 10.1109/tnb.2008.2011860

Lazcka, O., Del Campo, F. J., & Munoz, F. X. (2007). Pathogen detection: A perspective of traditional methods and biosensors. *Biosensors and Bioelectronics, 22*(7), 1205-1217. doi: 10.1016/j.bios.2006.06.036

Liu, J., & Lu, Y. (2006). Preparation of aptamer-linked gold nanoparticle purple aggregates for colorimetric sensing of analytes. *Nature Protocols, 1*(1), 246-252. doi: 10.1038/nprot.2006.38

Lonne, M., Zhu, G., Stahl, F., & Walter, J. G. (2014). Aptamer-modified nanoparticles as biosensors. *Advances in Biochemical Engineering/Biotechnology, 140*, 121-154. doi: 10.1007/10_2013_231

March, J. B. (2004). Improved formulations for existing CBPP vaccines recommendations for change. *Vaccine, 22*(31-32), 4358-4364. doi: 10.1016/j.vaccine.2004.03.066

Mei, Z., Chu, H., Chen, W., Xue, F., Liu, J., Xu, H., … & Zheng, L. (2013). Ultrasensitive one-step rapid visual detection of bisphenol A in water samples by label-free aptasensor. *Biosensors and Bioelectronics, 39*(1), 26-30. doi: 10.1016/j.bios.2012.06.027

Niu, S., Lv, Z., Liu, J., Bai, W., Yang, S., & Chen, A. (2014). Colorimetric aptasensor using unmodified gold nanoparticles for homogeneous multiplex detection. *PLoS One, 9*(10), e109263. doi: 10.1371/journal.pone.0109263

Petryayeva, E., & Krull, U. J. (2011). Localized surface plasmon resonance: Nanostructures, bioassays and biosensing--A review. *Analytica Chimica Acta, 706*(1), 8-24. doi: 10.1016/j.aca.2011.08.020

Song, K. M., Cho, M., Jo, H., Min, K., Jeon, S. H., Kim, T., … & Ban, C. (2011). Gold nanoparticle-based colorimetric detection of kanamycin using a DNA aptamer. *Analytical biochemistry, 415*(2), 175-181. doi: 10.1016/j.ab.2011.04.007

Song, K. M., Jeong, E., Jeon, W., Cho, M., & Ban, C. (2012). Aptasensor for ampicillin using gold nanoparticle based dual fluorescence-colorimetric methods. *Analytical and Bioanalytical Chemistry, 402*(6), 2153-2161. doi: 10.1007/s00216-011-5662-3

Stetefeld, J., McKenna, S. A., & Patel, T. R. (2016). Dynamic light scattering: a practical guide and applications in biomedical sciences. *Biophysical Reviews, 8*(4), 409-427. doi: 10.1007/s12551-016-0218-6

Tang, J., Wang, J. Y., & Parker, L. L. (2012). Detection of early Abl kinase activation after ionizing radiation by using a peptide biosensor. *Chembiochem, 13*(5), 665-673. doi: 10.1002/cbic.201100763

Zhang, Z., Li, H., Zhang, F., Wu, Y., Guo, Z., Zhou, L., & Li, J. (2014). Investigation of halide-induced aggregation of au nanoparticles into spongelike gold. *Langmuir, 30*(10), 2648-2659. doi: 10.1021/la4046447

Zhao, W., Chiuman, W., Lam, J. C., McManus, S. A., Chen, W., Cui, Y., … & Li, Y. (2008). DNA aptamer folding on gold nanoparticles: from colloid chemistry to biosensors. *Journal of the American Chemical Society, 130*(11), 3610-3618. doi: 10.1021/ja710241b

Zhou, H., Purdie, J., Wang, T., & Ouyang, A. (2010). pH measurement and a rational and practical pH control strategy for high throughput cell culture system. *Biotechnology Progress, 26*(3), 872-880. doi: 10.1002/btpr.369